Proceedings of the 2000 IEEE/RSJ International Conference on Intelligent Robots and Systems

Virtual Passive Dynamic Walking and Energy-based Control Laws

Fumihiko Asano
Dept. of Control Eng.
Tokyo Institute of Technology
2-12-1 Oh-okayama, Meguro-ku
Tokyo 152-8552, JAPAN
asano@ctrl.titech.ac.jp

Masaki Yamakita
Dept. of Mechanical and Control Eng.
Tokyo Institute of Technology
2-12-1 Oh-okayama, Meguro-ku
Tokyo 152-8552, JAPAN
yamakita@ctrl.titech.ac.jp

Katsuhisa Furuta
Dept. of Computers and Systems Eng.
Tokyo Denki University
Ishizaka, Hatoyama-cho, Hiki-gun
Saitama 350-0394, JAPAN
furuta@k.dendai.ac.jp

Abstract

It has been shown that a simplest walker with suitable parameter choice can walk down a gentle slope without any control forces and generate its steady walking pattern utilizing gravity effect automatically. On the floor, however, the robot cannot exhibit passive walk, so any application methods of passive walk to active walker on the horizontal floor has not been studied yet. Based on the observation, in this paper we introduce "virtual passive dynamic walking" with virtual gravity field which acts as a driving force for the biped robot. The robot can walk on the floor without any control torque except virtual gravity effect. Since the modified gravity field seems to be very close to real condition, the generated walking pattern seems to be natural. Further, multi-pattern walking w.r.t. energy level is proposed. With the proposed above method, safety and energy-effective control of biped walking robot can be realized.

1 Introduction

The study of bipedal walking in the framework of humanoid robots is recent active research area. The gait design problem is most important part of the legged robot control, however, many of them imitate human gait intuitively without any solid reasons which insure some optimality, especially energy consumptions.

On the other hand, the desired trajectories of walking robot are usually time-dependent. Since the controllers try to minimize the trajectory tracking error, very large force of actuators sometime occurs even if there exist human-being or some obstacles. Thus, in such cases the safety of control systems is not guaranteed any.

Based on the observation, in this paper we propose a safety and energy-effective control law based on passive dynamic walking originally studied by McGeer.[4] The passive walker generates its steady walking pattern automatically without any artificial control forces, so the gait seemed to be "natural" and energy-effective. On the floor, however, the robot cannot walk without any control forces. So we have introduced "virtual gravity field" toward the horizontal direction.[5] Then the robot can exhibit passive walking virtually utilizing only virtual gravity effect. We utilize its walking pattern as a desired motion of active walker which walks on the floor by actuators. And the controller based on virtual passive walk can realize the controlled system safety because it is *autonomous* system.

According to the above method, energy-effective and safety control for biped walking robot can be realized. The validity of control law is studied by numerical simulations and experiments.

2 Virtual Passive Dynamic Walking

2.1 The model and virtual gravity field

Fig. 1 shows the walking robot model. The model is compass-like biped robot which has actuators at ankle and hip joints, and the motion is assumed to be constrained to sagittal plane. The robot can walk on a gentle slope without using any actuators and the gait pattern converges 1-periodic stable limit cycle. On the level ground, however, the robot cannot walk without any control forces because there does not exist any driving force toward the walking direction. If small virtual gravity field toward the horizontal direction is

0-7803-6348-5/00/$10.00

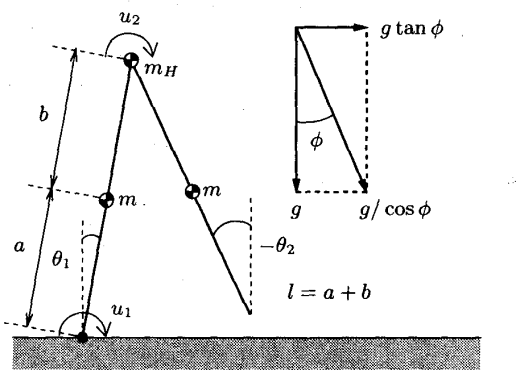

Figure 1: Model of the robot and virtual gravity field

exerted, the robot can exhibit *virtual passive* walking and the motion also converges 1-periodic stable limit cycle. The condition seemed to be on a gentle slope ϕ in the nominal gravity field $g/\cos\phi$. Since the value of ϕ is very small, this condition seemed to be very closed to real condition, so the gait pattern can be considered to be *natural*.

The dynamic equation during single support phase is given by

$$\boldsymbol{M}(\boldsymbol{\theta})\ddot{\boldsymbol{\theta}} + \boldsymbol{C}(\boldsymbol{\theta}, \dot{\boldsymbol{\theta}})\dot{\boldsymbol{\theta}} + \boldsymbol{g}(\boldsymbol{\theta}, \phi) = \boldsymbol{0}, \tag{1}$$

where $\boldsymbol{\theta} = \begin{bmatrix} \theta_1 & \theta_2 \end{bmatrix}^T$ is the coordinates of the configuration of the robot, $\boldsymbol{M}(\boldsymbol{\theta}) = [2 \times 2]$ is the inertia matrix, $\boldsymbol{C}(\boldsymbol{\theta}, \dot{\boldsymbol{\theta}}) = [2 \times 2]$ is colioris matrix and $\boldsymbol{g}(\boldsymbol{\theta}, \phi) = [2 \times 1]$ is gravity matrix. Please notice that $\phi = 0$ in the case of the real robot walking on the floor with control forces. The heel-strike collision is assumed to be inelastic and without sliding. The stance and swing legs switch during transition. Please see [6] for the detail. In this paper, we set the values of physical parameters as shown in Table 1 in the numerical simulations.

Table 1: Notations and numerical settings

m	leg mass	5.0	kg
m_H	hip mass	10.0	kg
a	lower part of the leg	0.50	m
b	upper part of the leg	0.50	m
l	leg length ($= a + b$)	1.00	m
g	gravity acceleration	9.81	m/sec^2
ϕ	virtual slope		rad
θ_1	stance leg angle w.r.t. vertical		rad
θ_2	swing leg angle w.r.t. vertical		rad
u_1	ankle torque		Nm
u_2	hip torque		Nm

2.2 Virtual energy and bifurcations

Here, we consider "virtual energy" which is total energy of the robot defined in the modified gravity field. Virtual energy E_V is sum of kinetic energy and potential energy in the modified gravity field, that is,

$$E_V(\boldsymbol{\theta}, \dot{\boldsymbol{\theta}}, \phi) = K_V(\boldsymbol{\theta}, \dot{\boldsymbol{\theta}}) + P_V(\boldsymbol{\theta}, \phi) \tag{2}$$

where K_V and P_V are defined as follows:

$$\begin{aligned} K_V(\boldsymbol{\theta}, \dot{\boldsymbol{\theta}}) &= K(\boldsymbol{\theta}, \dot{\boldsymbol{\theta}}) = \frac{1}{2}\dot{\boldsymbol{\theta}}^T \boldsymbol{M}(\boldsymbol{\theta})\dot{\boldsymbol{\theta}} && (3) \\ &= \frac{1}{2}(m_H l^2 + ma^2 + ml^2)\dot{\theta}_1^2 + \frac{1}{2}mb^2\dot{\theta}_2^2 \\ &\quad -mbl\cos(\theta_1 - \theta_2)\dot{\theta}_1\dot{\theta}_2 && (4) \\ P_V(\boldsymbol{\theta}, \phi) &= (m_H l + ml + ma)\cos(\theta_1 + \phi)\frac{g}{\cos\phi} \\ &\quad -mb\cos(\theta_2 + \phi)\frac{g}{\cos\phi} && (5) \end{aligned}$$

The system becomes virtually passive w.r.t. E_V. In other words, E_V is kept constant in the case without any external energy sources. Fig. 3 shows the simulated result of virtual energy vs. time. The robot started from some initial condition near steady initial condition and virtual energy converges constant value as well as its walking pattern. For higher values of virtual slope, the compass-gait exhibits *period-doubling* bifurcation. Fig. 2 shows the phenomena in virtual energy. The behavior becomes chaotic near 0.090 [rad] and for more larger virtual slope the robot cannot walk. This phenomena is similar to that of passive dynamic walking.[1][9][10]

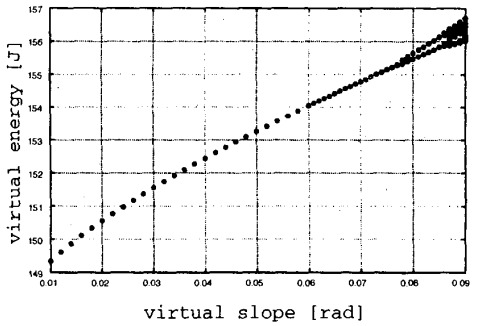

Figure 2: Chaos in virtual energy

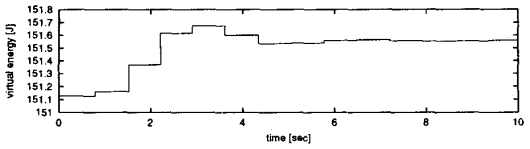

Figure 3: Virtual energy vs. time ($\phi = 0.03$ [rad])

3 Active Walking

The dynamic equation of the real robot on the level:

$$\boldsymbol{M}(\boldsymbol{\theta})\ddot{\boldsymbol{\theta}} + \boldsymbol{C}(\boldsymbol{\theta}, \dot{\boldsymbol{\theta}})\dot{\boldsymbol{\theta}} + \boldsymbol{g}(\boldsymbol{\theta}) = \boldsymbol{\tau} + \boldsymbol{\tau}_e \qquad (6)$$

where $\boldsymbol{\tau} = \boldsymbol{S}\boldsymbol{u}$ is control input and $\boldsymbol{\tau}_e$ is the environmental forces. We can transform the virtual gravity effect to actuator torque at hip and ankle as shown in Fig. 4 which is given by

$$\boldsymbol{\tau} = \boldsymbol{S}\boldsymbol{u} = \begin{bmatrix} 1 & 1 \\ 0 & -1 \end{bmatrix} \begin{bmatrix} u_1 \\ u_2 \end{bmatrix} \qquad (7)$$

$$= \begin{bmatrix} (m_H l + ml + ma)\cos\theta_1 \\ -mb\cos\theta_2 \end{bmatrix} g\tan\phi, \qquad (8)$$

and torque of ankle and hip are given by:

$$u_1 = (m_H l + ml + ma)g\cos\theta_1\tan\phi - mbg\cos\theta_2\tan\phi, \qquad (9)$$

$$u_2 = mbg\cos\theta_2\tan\phi. \qquad (10)$$

Here, please notice that $\boldsymbol{\tau} = \boldsymbol{\tau}(\boldsymbol{\theta}, \phi)$ depend only on angular positions and virtual slope, does not depend on time. Since the control input is determined by only positional information, the control system is *autonomous* system.

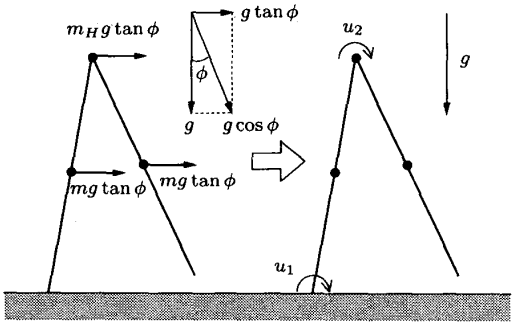

Figure 4: Torque transformation

Fig. 5 shows the simulated results of actuator torque vs. time where $\phi = 0.03$ [rad]. The control is assumed to be implemented as a digital controller, i.e., Z.O.H. is introduced in front of the actuator, where the control interval is 1.0 [msec]. We can see that the torque is almost constant. The constant-like torque is special feature of passive or virtual passive walking and it can be an indicator of "*natural motion*". Further, the flatness of $\boldsymbol{\tau}$ implies that of $\boldsymbol{u}$. According to the small change of $\boldsymbol{u}$, the change of ZMP(Zero-Moment Point)[3] also becomes small and this is special property of virtual passive walk.

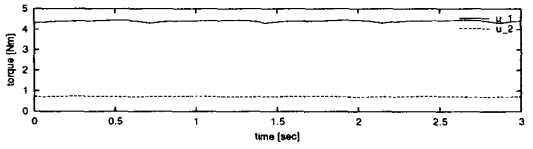

(a) torque

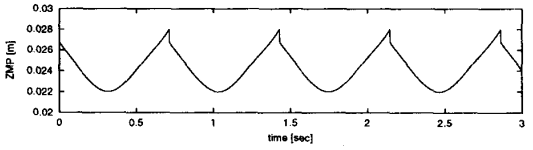

(b) ZMP

Figure 5: Torque and ZMP vs. time

4 Experiments

In order to check the validity of the proposed method, we constructed an experimental system. In this section, we explain the experimental set-up and show the results.

4.1 The experimental machine

In Fig. 6 we show the experimental machine. The robot has straight legs of the same length and three DC motors with encoders at hip position. The ankle joints are driven by tinning belts. Because of the symmetric structure the motion is constrained to sagittal plane and as a result the robot can be regarded as a two-legged robot as shown in Fig. 1.

4.2 Model following control using VIM

In this section, we consider model following control of the motion generated by VIM(Virtual Internal

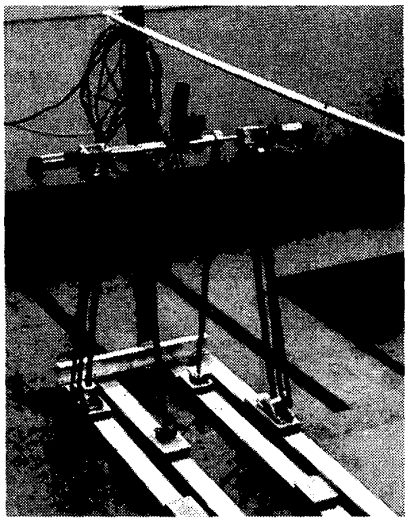

Figure 6: Experimental machine and floor

Model)[11] which is a reference model driven by sensory information. By the use of VIM, the some uncertainties of identification which is crucial factor in the case of model matching control can be compensated for. The dynamic equation of VIM with virtual control input is given by

$$\hat{\boldsymbol{M}}(\boldsymbol{\theta})\ddot{\boldsymbol{\theta}} + \hat{\boldsymbol{C}}(\boldsymbol{\theta},\dot{\boldsymbol{\theta}})\dot{\boldsymbol{\theta}} + \hat{\boldsymbol{g}}(\boldsymbol{\theta}) = \hat{\boldsymbol{\tau}}(\boldsymbol{\theta},\phi). \quad (11)$$

And the resultant control input for model following control of the real robot is given as

$$\boldsymbol{\tau} = \hat{\boldsymbol{M}}(\boldsymbol{\theta})\boldsymbol{u} + \hat{\boldsymbol{C}}(\boldsymbol{\theta},\dot{\boldsymbol{\theta}})\dot{\boldsymbol{\theta}} + \hat{\boldsymbol{g}}(\boldsymbol{\theta}) \quad (12)$$

$$\boldsymbol{u} = \ddot{\boldsymbol{\theta}}_d + \boldsymbol{K}_D(\dot{\boldsymbol{\theta}}_d - \dot{\boldsymbol{\theta}}) + \boldsymbol{K}_P(\boldsymbol{\theta}_d - \boldsymbol{\theta}) + \boldsymbol{K}_I \int (\boldsymbol{\theta}_d - \boldsymbol{\theta})dt. \quad (13)$$

By the use of this nonlinear feedback, the biped robot's dynamics is linearized. In this case, the closed loop system is also autonomous system. The ankle joint of the swing leg is controlled by PID controller in order to keep the foot posture horizontal.

4.3 Experimental results

Fig. 7 shows the experimental results. In the experiment the control period was set to 2 [msec] and the angular velocity was measured through a filter whose transfer function is $70/(s+70)$ for each actuator. The dynamic parameters of the robot were identified offline as: $m = 0.40$ [kg], $m_H = 3.0$ [kg], $l = 0.68$ [m], $a = 0.215$ [m] and $b = 0.465$ [m]. We set the input saturation function as $|u_i| \leq 0.60$ [Nm] where $u_1 = \tau_1 + \tau_2, u_2 = -\tau_2$. The virtual energy and ZMP are calculated by the information of VIM. From (c) and (d), it can be seen that although the control input and ZMP oscillate severely during the transition instant, during almost of the swing phase they keep small range. The ankle torque u_1 is very large due to pushing force at start. The reason why there are some differences between simulated control input and actual one is modeling error of VIM in dynamic parameters and frictions. (e) shows the virtual energy vs. time. Although during the saturated phase virtual energy is not kept constant value, constant energy is realized in other phase.

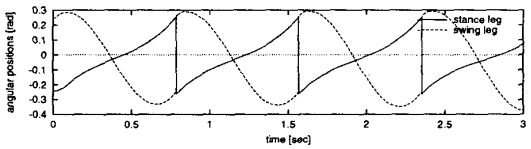

(a) angular positions

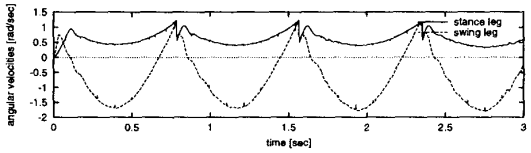

(b) angular velocities

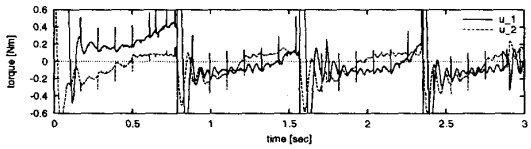

(c) torque

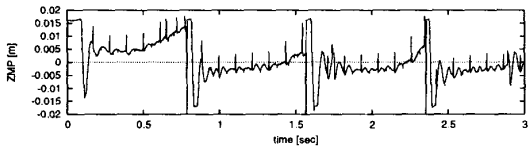

(d) ZMP

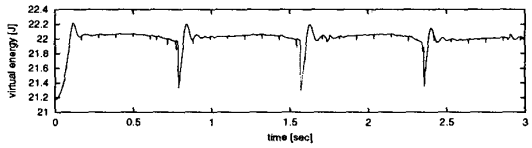

(e) virtual energy

Figure 7: Experimental results

5 Some Extensions

5.1 Knees and MVGF formulations

In this section, we investigate virtual passive walk in the presence of knee-joint. The kneed robot is essentially identical with compass-gait biped, that is, the compass model have the knee joint locked. Fig. 8 shows the model of kneed biped. The dynamics of kneed robot is more complex than the compass and its steady gait cannot be obtained easily without suitable parameter choice. Based on the observation, we propose MVGF(Multi-Virtual Gravity Field) for the robot in order to create steady walking pattern without loss of virtual passivity. In this case, the virtual potential energy can be defined as

$$P_V(\boldsymbol{\theta}, \phi_H, \phi_1, \phi_2, \phi_3) = \frac{J_H g}{\cos\phi_H} + \sum_{i=1}^{3} \frac{J_i g}{\cos\phi_i}$$

where

$$\begin{aligned} J_H &= m_H l_1 \cos(\theta_1 + \phi_H) \\ J_1 &= m_1 a_1 \cos(\theta_1 + \phi_1) \\ J_2 &= m_2(l_1 \cos(\theta_1 + \phi_2) - b_2 \cos(\theta_2 + \phi_2)) \\ J_3 &= m_3(l_1 \cos(\theta_1 + \phi_3) - l_2 \cos(\theta_2 + \phi_3) \\ &\quad -b_3 \cos(\theta_3 + \phi_3)) \end{aligned}$$

and virtual kinetic energy is given by $K_V(\boldsymbol{\theta}, \dot{\boldsymbol{\theta}}) = K(\boldsymbol{\theta}, \dot{\boldsymbol{\theta}}) = \frac{1}{2}\dot{\boldsymbol{\theta}}^T \boldsymbol{M}(\boldsymbol{\theta})\dot{\boldsymbol{\theta}}$, then total virtual energy is kept constant in the case without any external energy sources. The constant-like torque is also realized. The transformed torque is given by

$$\boldsymbol{\tau}(\boldsymbol{\theta}, \phi_H, \phi_1, \phi_2, \phi_3) = \begin{bmatrix} \cos\theta_1 & & \\ & \cos\theta_2 & \\ & & \cos\theta_3 \end{bmatrix} \times \begin{bmatrix} m_H l_1 & m_1 a_1 & m_2 l_1 & m_3 l_1 \\ & & -m_2 b_2 & -m_3 l_2 \\ & & & -m_3 b_3 \end{bmatrix} \begin{bmatrix} g\tan\phi_H \\ g\tan\phi_1 \\ g\tan\phi_2 \\ g\tan\phi_3 \end{bmatrix}.$$

5.2 Multi-pattern walking

The virtual energy can be a parameter of the walking pattern. In other words, the gait can be modified w.r.t. its energy level. First, let us consider in the case of compass-gait biped with single virtual gravity effect. The controlled virtual slope is given by

$$\phi(E_V) = \eta(E_V)\phi^{\text{low}} \quad (14)$$

$$\eta(E_V) = \frac{\gamma + \exp(-\zeta(E_V - \bar{E}_V))}{1 + \exp(-\zeta(E_V - \bar{E}_V))} \quad (15)$$

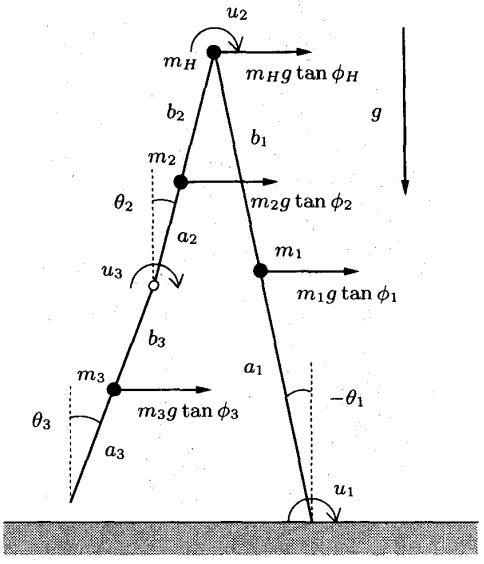

Figure 8: Model of kneed biped and multi-virtual gravity effect: $m_H = 10.0, m_1 = 5.0, m_2 = 3.0, m_3 = 2.0$ [kg], $l_1 = 1.0, l_2 = l_3 = 0.5, a_1 = 0.4, a_2 = 0.1, a_3 = 0.15$ [m]

$$\bar{E}_V = \frac{1}{2}\left(E^{\text{high}} + E^{\text{low}}\right) \quad (16)$$

$\bar{E}_V$ is the mean value between two energy levels and γ is the ratio of two slopes, that is, $\gamma = \phi^{\text{high}}/\phi^{\text{low}}$. Then multi-pattern walking is realized.

Next, in the case of kneed-biped, since the kinetic energy of the kneed biped dissipates at knee-strike instant, virtual energy also dissipates. So we must consider mean values of virtual energy of 3-link and 2-link mode in each energy level, that is,

$$\bar{E}_V = \frac{1}{2}\left(\bar{E}^{\text{high}} + \bar{E}^{\text{low}}\right)$$

where $\bar{E}^{\text{high}}$ denotes mean value of E_V between 3-link and 2-link in high-energy level motion and $\bar{E}^{\text{low}}$ denotes that of in low-energy level. Further, in the case of MVGF formulation, we must set the functions of virtual slopes each other. In this paper, the virtual slopes are defined by

$$\phi_H(E_V) = \eta(E_V)\phi_H^{\text{low}}, \quad \phi(E_V) = \eta(E_V)\phi^{\text{low}}$$

where $\phi = \phi_1 = \phi_2 = \phi_3$ and γ is the ratio of two slopes, that is, $\gamma = \phi_H^{\text{high}}/\phi_H^{\text{low}} = \phi^{\text{high}}/\phi^{\text{low}}$.

5.3 Numerical simulations

Fig. 9 shows the simulated result with external force. The all simulated situations are identical with the previous ones. We set $\phi_H^{\text{low}} = 0.025, \phi^{\text{low}} = 0.040$ and $\phi_H^{\text{high}} = 0.0325, \phi^{\text{high}} = 0.052$. Thus, $\gamma = 1.30$. The biped robot is pushed forward by a force 5.0 [N] at the hip position for the duration of 0.1 [sec] (from 2.0 to 2.1 [sec]). From Fig. 9, we can see that the virtual energy increases and then the virtual slopes also increase. The walking pattern slides and converges new one automatically without any reaction forces because there are not any desired trajectory.

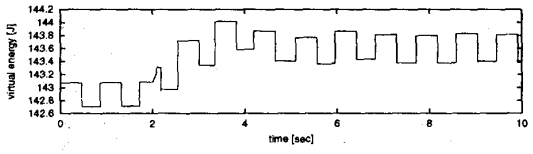

(a) virtual energy vs. time

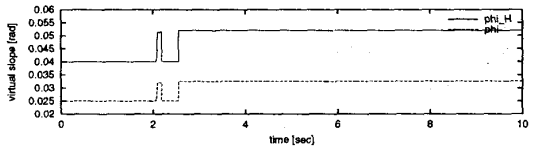

(b) virtual slope vs. time

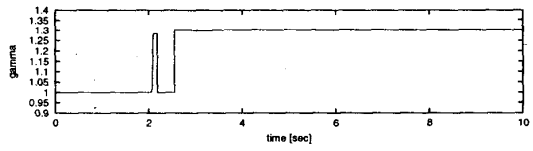

(c) γ vs. time

Figure 9: Simulated results of multi-pattern walking

6 Conclusions

In this paper, we have proposed a virtual passive dynamic walking with virtual gravity field and checked the validity of the proposed method by numerical simulation and experiments. Since the controlled system is autonomous system, the walking motion is safe to human-being and some obstacles. Further, an extended method which can change and create the walking motion automatically w.r.t. virtual energy levels has proposed. In the future, we should apply the method for humanoid robots which has the upper half of the body.

Acknowledgment

This research is supported by The Grant-in Aid for COE Research Project of Super Mechano-System by the Ministry of Education, Science, Sport and Culture. The authors acknowledge the support by Mr. Minoru Hashimoto and Mr. Norihiro Kamamichi.

References

[1] A. Goswami, B. Thuilot, and B. Espiau, "A Study of the passive gait of a compass-like biped robot: symmetry and chaos," *The Int. J. of Robotics Research*, Vol. 17, No. 15, pp. 1282-1301, 1998.

[2] A. Goswami, B. Espiau and A. Keramane, "Limit cycle in a passive compass gait biped and passivity-mimicking control laws," *Autonomous Robots*, Vol. 4, No. 3, pp. 273-286, 1997.

[3] A. Goswami, "Postural stability of biped robots and the foot-rotation indicator(FRI) point," *The Int. J. of Robotics Research*, Vol. 18, No. 6, pp. 523-533, 1999.

[4] T. McGeer, "Passive dynamic walking," *The Int. J. of Robotics Research*, Vol. 9, No. 2, pp. 62-82, 1990.

[5] F. Asano, M. Yamakita and K. Furuta, "Stabilizing control of passive biped robots and its application to active walking," *The Fifth Int. Symp. on Artificial Life and Robotics*, Vol.2, pp. 503-506, 2000.

[6] M. Yamakita, F. Asano and K. Furuta, "Passive velocity field control of biped walking robot," *IEEE Int. Conf. on Robotics and Automation*, Vol. 3, pp. 3057-3062, 2000.

[7] K. Osuka and K. Kirihara, "Motion analysis and experiments of passive walking robot QUARTET II," *IEEE Int. Conf. on Robotics and Automation*, Vol. 3, pp. 3052-3056, 2000.

[8] Mark W. Spong, "Passivity based control of the compass gait biped," *14th World Congress of IFAC*, pp. 19-23, 1999.

[9] G. W. Howell and J. Baillieul, "Simple controllable walking mechanisms which exhibit bifurcations," *The 37th IEEE Conf. on Decision and Control*, Vol. ?, pp. 3027-3032, 1998.

[10] M. Garcia, A. Chatterjee, A. Ruina and M. Coleman, "The simplest walking model: stability, complexity, and scaling," *ASME J. of Biomechanical Engineering*, Vol. 120, pp. 281-288, 1998.

[11] K. Kosuge, J. Ishikawa, K. Furuta and M. Sakai, "Control of single-master multi-slave manipulator system using VIM," *IEEE Int. Conf. on Robotics and Automation*, Vol. 3, pp. 1172-1177, 1990.